Multi-feature learning adaptive network for underwater image enhancement

ABSTRACT

Underwater image enhancement faces variety of challenges owing to the diversity of underwater scenes(viewed as water types) and the rich multi-frequency information.To deal with these challenges, this paper proposes a multi-feature learning adaptive underwater image enhancement network comprising an adaptive module and a dual-layer synchronous enhancement network.First, we design an adaptive module which enables the determination of water type inside the model and eliminates thenegative effect of water type diversity by building water type related features.Then, the model learns high-frequency and low-frequency features through a dual-layer synchronous enhancement networkto extract more comprehensive information.Finally, the outputs of the dual-layer network are merged to obtain more realistic underwater enhanced images.Numerous experiments have shown that the proposed method outperforms the comparison method for visual perception and assessment metrics.

Keywords: Underwater Image, Image Enhancement; Deep Learning, Multi-frequency Information.

1. INTRODUCTION

Underwater imagery is an important toolfor obtaining marine information and plays an essential role in the field of marine research and underwater robotics. However,the light suffers severe attenuation and scattering during it propagates underwater.Complex underwater imaging processes lead to low contrast, color distortion and blurred details in underwater images. Besides,different underwater scenes, namely water types, have different effects on degraded images. However, many existing studies on underwater image enhancement have not specifically focused on addressing the effects of different water types.In addition, underwater images contain rich information that can be simply divided into low-frequency and high-frequency components.High-frequency components refer to local information, mainly consisting of texture and noise details in the image.Conversely, low-frequency components mainly contain global information within the color and structure.

In this paper, we propose a multi-feature learning adaptive underwater image enhancement network to solve the effects of different water types and multi-frequency features on underwater image enhancement. The proposed network primarily comprises two parts: an adaptive module and a dual-layer synchronous enhancement network.The adaptive module is able to adaptively cope with the interference caused by different water types to the degraded images, preserving the features relevant to the scene.The network employs two branches to learn high-frequency and low-frequency features, integrating attention operation [1] with different receptive fields to ensure synchronized extraction of local features and modeling of long-term dependencies for enhanced image quality.This methodallows for a

more nuanced analysis of the image content, andmakes the color and detail of the enhanced result closer to ground truth, compared with the previous model.

2. RELATED WORK

At present, underwater image enhancement methods can be divided into underwater image enhancement and underwater image restorationdepending on the way in which the image is processed underwater.

2.1 UNDERWATER IMAGE ENHANCEMENT METHOD

The underwater image enhancement method does not need to consider the image formation process, and directly processes the pixels of the underwater image to improve visual perception. Jamadandi et al. [2] proposed a deep learning structure based on Wavelet correction transformation. By using Wavelet correction transformation structure, image enhancement is regarded as a problem of image style transformation. Islam et al. [3] formulated the problem as image-to-image conversion, and conducted confrontational training on a large number of data sets based on the GAN model to learn the mapping. Li et al. [4] proposed water-NET to maintain degraded image features and obtain enhanced images by taking histogram equalization, white balance, and gamma correction into account. Uplavikar et al. [5] made an attempt to confirm water type, and learned the features of images by separating unnecessary interference with water types. However, the network structure pays more attention to the characteristic information. Meanwhile, the obtained water type is often inaccurate. Thus, the network tends to introduce color distortion around the edges. Recently, Transformer shines in the field of computer vision. Peng et al. [6] introduced the Transformer model into the task of underwater image enhancement, and combined CNN with Transformer, which can not only model long-term dependence relationships but also pay attention to local information. zhou et al. [23] effectively solved the problems of poor visibility and feature drift of underwater images through a multi-interval sub-histogram perspective equalization underwater image enhancement method, which significantly improved the visual effect and performance of underwater images.

The aboved researches typically employed a single-branch network toenhcane the destoryed image.This structure leads to information disorder when handling various semantic information, resulting in weaknesses in processing multi-frequency information. To address this issue, we introduce a dual-branch synchronous enhancement network where two branches independently decode information of different frequencies to enhance the model's capacity in extracting multi-frequency information.

2.2 UNDERWATER IMAGE RESTORATION METHOD

The purpose of the image restoration method is to solve the serious degradation of the underwater image caused by the scattering of underwater light, other complex underwater imaging environments, such as low contrast, color decay and distortion [7]. Li et al. [8] propose a deep underwater image restoration model combined with the attention mechanism, integrating the characteristics of the different color spaces, to solve the underwater image color deviation and the problem of low contrast. Chiang et al. [9] proposed wavelength compensation and image de-fog algorithm (WCID). This model considers removing light scattering and color change caused by the possible artificial light source, and compensating for the difference in wavelength attenuation when crossing water depth to the top of the image. Thus, it can eliminate the distortion caused by light scattering and color change. Since attenuation caused by wavelength changes leads to asymmetric propagation

of colors, PrasenSharma et al. [10] proposed to select corresponding receptive fields based on channel propagation range to suppress irrelevant semantic features, and improve model performance. According to the characteristics of underwater imaging, Drews [11] proposed underwater dark channel Prior (UDCP) to correct background light by combining dark channel Prior (DCP) [12] with color saturation. DCP is used to process ground images, but it has almost no effect on underwater images. UDCP cannot correctly restore scenes of underwater images. Anwar et al. [13] synthesized ten different types of underwater images for training according to the light attenuation coefficients of red, green, and blue in water with the different depths. The underwater image restoration method takes into account different imaging characteristics, but it is hard to calculate too many imaging parameters.Zhou et al. [24] proposed multicolor components and light attenuation (MCLA), whichutilizes adaptive background light estimation, depth-map enhancement, and transmission map computation to effectively restore color, detail, and visibility in underwater images. Hou et al. [25] introduced the illumination channel sparsity prior (ICSP) guided variational framework for non-uniform illumination underwater image restoration, leveraging the illumination channel sparsity prior and a variational model with L0 norm term, constraint term, and gradient term to enhance the quality of images.

Although the above methods demonstrate good performance in certain scenarios, they require redesign when confronted with new situations. To enhance the model's generalization, we introduce an adaptive module to assess the water type within the input image and enhance underwater images within a specific domain.

Our proposed model is able to deal well with the impacts of different water types and capture more comprehensive information, achieving state-of-the-art results on real-world [4] [8] [9] and synthetic datasets [14].

3. METHOD

The proposed multi-feature learning adaptive underwater image enhancement framework is shown in Figure.1, the framework consists of two parts, adaptive module to remove the influence of water type on the generated images, and dual-layer synchronous enhancement network to learn features of different frequencies.

3.1 Adaptive module

The quality of underwater images is degraded due to wavelength-dependent light absorption and scattering in underwater scenes. Besides,underwater images captured from different domain scenes vary in brightness, contrast and visibility. It is difficult to accurately enhance underwater images from different underwater scenes using traditional networks.Hence,we expect our model could recognize the difference information of underwater images, so that the model can be more targeted to reconstruct clear images in specific water types. To address this problem, we propose an adaptive module (AM), which consists of water type classifier and water type related feature extractor, as shown in Figure 1 (b).Next, we will carefully describe each component.

As shown in Figure 1 (a), The encoder adopts the degraded image as input to obtain the compression encoded features. Although the encoded features contain most of the feature information in an underwater image, the information related to the water types is not sufficient and may lead to erroneous enhancements during processing of the image. Therefore, we apply the encoded feature as the input of adaptive module to further extract the water type related information. The water type classifier identifies the water type based on the encoded feature. As shown in Figure 1 (c), the water type classifier consists of convolutional layer, batch normalization, ReLUactivation function and linear layer.This

structure effectively improves the performance of the model andreduces the computational cost.The water type classifier can be defined as followed:

$$I, I^{'} = C(E(X)) \quad (1)$$

where$X$ is the input image, $C(\cdot)$ and $E(\cdot)$ denote the water type classifier and encoder.I is used to determine the water type of the input image, and $I^{'}$ is the output of the middle layer of the classifier.

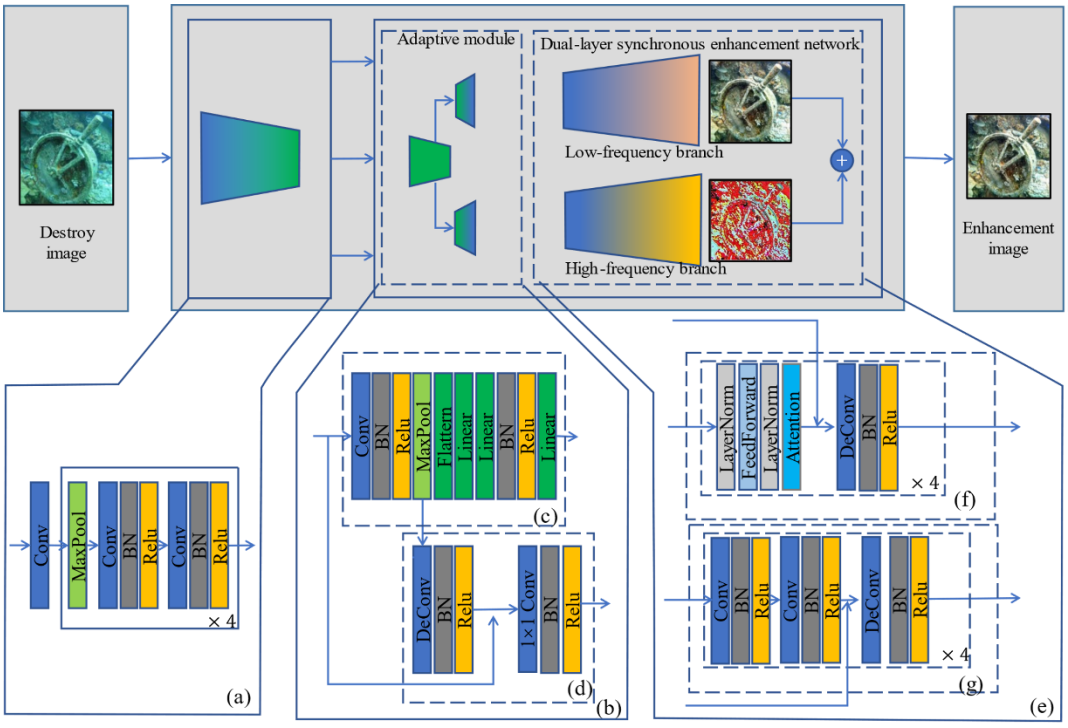

Figure. 1.The framework consists of three parts: (a) the encoder consists of a series of convolutional blocks; (b) an adaptive moduleconsists of (c) water type classifier and (d) water type related feature extractor, which be used to separate the interference of water types; (e) a dual-layer synchronization network consists of (f)low-frequency branch and (g) high-frequency branch for learning high-frequency and low-frequency information separately.

Since the encoded features lack sufficient features related to the water type, which leads to disordered information in the decoding process. Thus,we add a water type related feature extractor to get the information relatedto water typeby combine the encoded feature and$I^{'}$.Specifically,the output of the middle layer of the classifier contains information related to the water type,we employ deconvolutional implementation to upsample it.The upsampled features mostly contain water type information and are weakly correlated with other semantic information in the image. Hence, we perform an element-wise additionoperation on the middle layer features and the encoded features, and then use point-wise convolution to obtain water type related features. This process can be defined as follows:

$$\bar{I} = Conv_{1\times1}(DeConv(I^{'})E(X)) \quad (2)$$

where $DeConv(\cdot)$and $Conv_{1\times1}(\cdot)$denote deconvolutional layer and point-wise convolution, both of them arefollowed by batch normalization and ReLUactivationfunction. $\bar{I}$ is the water type related feature, whichused as the input of the subsequent dual-layer synchronous enhancement network.

Through this module, it can adaptively remove the influence on the reconstructed image caused by the diversity of water types in the degraded image with different watercolors, and enhanced the generalization ability of the model.

3.2Dual-layer synchronous enhancement network

Most of the traditional underwater image enhancement networks do not consider the feature information at different frequencies underwater, resulting in enhanced images that still have detail loss. Underwater images are rich in feature information, and features of different frequencies contribute differently to the enhanced images.

Underwater images mainly contain high-frequency information with obvious changes of detailed features such as line and noise, and low-frequency information such as color and texture. In order to learn these features more comprehensively, we propose a dual-layer synchronous enhancement network. The proposed dual-layer synchronous enhancement network is composed of two identical layers, high-frequency branch (HF Branch)and low-frequency branch (LF Branch) and its structure is shown in Figure. 1 (e). The two identical branches withdifferent respective fieldsto generate high-frequency and low-frequency images.The complex imaging environment of underwater images leads to blurred edges of underwater images and generates a lot of noise. Therefore, we use high-frequency branch which implemented by convolution to reconstruct local detail information.The base feature extractblock of the high-frequency branch can be represented as follows:

$$X_i^{\mathrm{H}} = \mathrm{DeConv}(Concat(\mathrm{Conv}_2(\mathrm{Conv}_1((X_{i-1}\text{^})), \bar{X}_{i-1})) \quad (3)$$

where i is the number of layers of high-frequency branch, andX_0 is the water type related feature, and $\bar{X}_{i-1} = \bar{I}$ when $i = 1$. $\mathrm{Conv}(\cdot)$ denotes convolutionalfollowed by batch normalization and ReLUactivation function.Additionally, the feature maps are too coarse to provide more accurate detail information due to multiple downsampling.Therefore, we incorporate skip connections $Concat(\cdot)$ between the corresponding sampling levels to facilitate easier model training.This branch helps the model remove noise while enhancing the sharpness of the edges in the enhanced results.

Morever,due to the effects of underwater light refraction and scattering, a large amount of energy is lost when the light is transmitted to the camera, resulted in color shift and structure blurred global information destroyed during imagingAlthough CNN is good at processing images, it is weak at long-range modeling of features. Fortunately, it has been recently shown that global attention in Multi-headed Selfattention in Transfromer can effectively capture low-frequency information [15].Hence, we use low-frequency branch embedded with attention operation to learn global information, as shown in Figure. 1 (f).The base feature extractblock of the low-frequency branch can be represented as follows:

$$LF_i(X_{i-1}) = DeConv(Concat(Att(LN(FFD(LN((X_{i-1})))), \bar{X}_{i-1})) \quad (4)$$

Where $LN(\cdot)$ and $FFD(\cdot)$ denote layer normalization and feed forward network, and$Att(\cdot)$represents attention operation.This branch further enhances the similarity between each color space of the output image and ground truth.

The dual-layer synchronous enhancement network is capable of learning information at different frequencies, reconstructing structural information. The final output is created by the elemental addition of the outputs of the two branches.

3.2Train loss

Our train loss consists of two parts, one is used to Train the cross-entropy loss of water type, and the other is image enhancement loss.

3.2.1 Cross-entropy Loss

We calculate the cross entropy between the predicted water type and the target water type to train the classifier and improve the prediction accuracy. The cross-entropy loss is as follows:

$$L_C(I, C) = -\sum_{c=1}^{M} y_c log I_c \quad (5)$$

Here, I is the output of the classifier, C is the real water type and c is the classifier predicted water type. $y_c = 1$ if $C = c$, i.e., when the classifier predicts the correct water type, otherwise $y_c = 0$.

3.2.1 Reconstruction Loss

To ensure that the rendering effect of the generated image is closer to ground truth, we propose an aggregation loss. The proposed reconstruction loss is defined as follows:

$$L_R(Y, Y_G) = \alpha L_{\text{SSIM}}(Y, Y_G) + \beta L_{Color}(Y, Y_G) + \gamma L_{MSE}(Y, Y_G) \quad (5)$$

where α,β,γ represent the proportional coefficients of each loss component,we set them to 0.4, 0.4, and 0.2.L_{SSIM} , L_{Color} and L_{MSE} aredescrible as follows.

Structual similarity (SSIM) loss function is able to evaluate well the brightness, contrast and structure of the generated image, so it is used to learn both of high- and low-frequency information. Theloss function is as follows:

$$L_{SSIM}(Y, Y_G) = 1 - \frac{(2\mu_Y \mu_{Y_G} + C_1)(\sigma_{YY_G} + C_2)}{(\mu_Y^2 + \mu_{Y_G}^2 + C_1)(\sigma_Y^2 + \sigma_{Y_G}^2 + C_2)} \quad (7)$$

Where Y is the enhancement image, Y_G is theground truth image. μ_Y and σ_Y denote the enhancedresult mean and standard deviation, μ_{Y_G} and σ_{Y_G} denote the ground truth mean and standard deviation. σ_{YY_G} is the covariance between the enhanced image and the ground truth. In this study, we set $C_1 = C_2 = 1e - 5$, which is used to prevent the denominator from being zero.

Inspired by [7], we calculate the color difference of different channels between the lowfrequency feature image and ground truth, which is used to learn color information, the loss function is given as

$$L_{color}(Y, Y_G) = \|0.4\Delta R^2 + 0.4\Delta G^2 + 0.2\Delta B^2\|_2 \quad (8)$$

where ΔR, ΔG, ΔB represents the color difference between different channels in RGB color space.

MSE loss is used to calculate the reconstruction loss between the clear image and the enhanced image. It is defined as follows:

$$L_{MSE}(Y, Y_G) = \|Y - Y_G\|_2^2 \quad (9)$$

4. EXPERIMENT

Our model is implemented by the PyTorch framework on a Windows 10 workstation equipped with an NVIDIA GTX2070 GPU. We train the proposed model on real world dataset [4] and synthetic dataset [14] with a total of 10K pairs of underwater images and 300 epoches of training. We conduct extensive experiments in various dataset to explore the effectiveness of the proposed model.we compare the proposed model with several representative approach, includingIBLA [17], UDCP [18], ULAP[19], RGHS [20], CycleGAN[21], SESR[3], DAL[5].Besides, ablation studies are conducted to demonstrate the advantages of each component in our model.

We use two evaluation metrics, SSIM [26] andPeak Signal to Noise Ratio(PSNR) [27], to objectively assess the enhancement performance of the model.SSIM is defined as:

$$SSIM(Y,Y_G)=\frac{(2\mu_Y\mu_{Y_G}+C_1)(\sigma_{YY_G}+C_2)}{(\mu_Y^2+\mu_{Y_G}^2+C_1)(\sigma_Y^2+\sigma_{Y_G}^2+C_2)} \quad (10)$$

here, the means of each symbol in this formula are the same as in Eq.(7). The formula of PSNRis detailed as follows:

$$PSNR(Y,Y_G)=10\times log_{10}\frac{255^2}{E_{MS}(Y,Y_G)} \quad (11)$$

$$E_{MS}(Y,Y_G)=\frac{1}{mn}\sum_{i=0}^{m-1}\sum_{n=0}^{n-1}\|Y(i,j)-Y_G(i,j)\|^2 \quad (12)$$

where E_{MS} represents the mean square error between the enhanced image Y and clear imageY_G mean square error.Higher values of SSIM and PSNR indicate that the image quality is closer to the clear image.

4.1Evaluation on real-world underwater images

We evaluate the proposed network and other methods in underwater images from UIEB [4]. The enhancement results of different methods are shown in Figure. 2, which shows the comparison results of underwater images with different watercolor tones. According to the comparison results, our model has favorable visual perception, and independent of water type. Table 1 lists the PSNR and SSIM values of comparisonmethods. The proposed method has the most competitive results in thesemetrics, indicating that our method is effective, can deal with the effects of underwater image degradation caused by different water types.

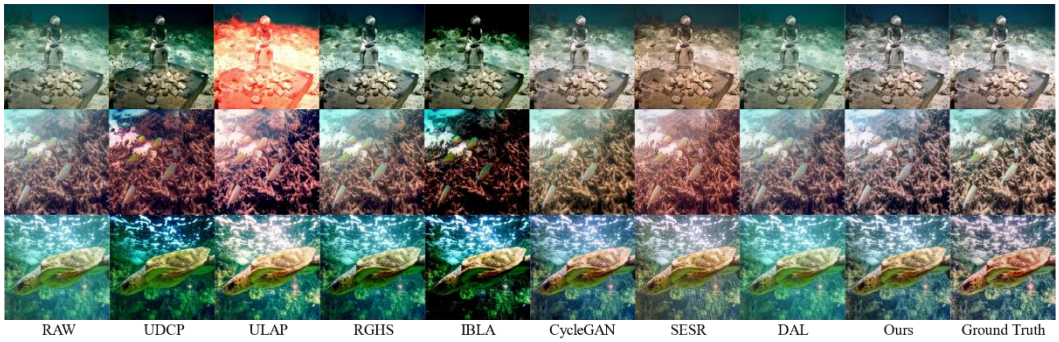

Figure 2. Qualitative comparisons of results on real-world underwater images.

Table 1. Underwater image quality evaluation of different variants of the presented method. Bold values show the best performer.

Metric	Raw	UDCP	ULAP	RGHS	IBLA	CycleGAN	SESR	DAL	Ours
PSNR	16.54	12.47	15.60	18.81	15.81	21.25	17.22	16.47	**25.00**
SSIM	0.78	0.57	0.70	0.81	0.71	0.85	0.78	0.75	**0.91**

To further validate the generality of the model, we use the UFO-120 [8], EUVP-Imagenet [9] and EUVP-Scenes [9] datasets (denoted by UFO, IGN and SC, respectively) as test evaluations. The visual results are shown in Figure. 3, and the PSNR and SSIM values are shown in Table 2. Compared with other methods, the proposed method shows excellent performance in terms of contrast enhancement and detail recovery.Both quantitative and qualitative results are sufficient to show that our method has good perceptual properties with high quality recovery results, and the trained model is capable of good generalization performance.

4.2Evaluation on synthetic underwater images

In this experiment, we evaluate the performance of synthetic underwater images for different water types. Figure. 4 presents the visual comparison for different methods. Compared with other methods, the proposed method effectively enhances the visibility of multiple water types, restores relatively realistic colors and details in very low visibility, and the processing results of the model are visually closer to clear images. Table 3 lists the average values of PSNR and SSIM in the synthetic underwater data set for eight water types. These quantitative results show that our proposed network achieves satisfactory results.

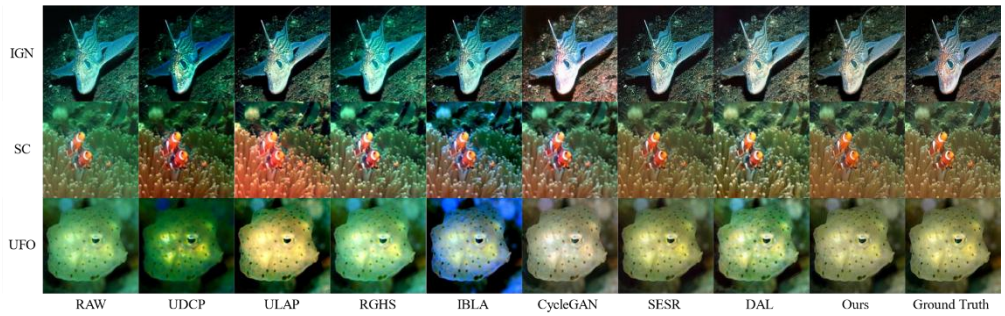

Figure 3. Qualitative comparisons of results on testreal-world underwater images.

Table 2. Underwater image quality evaluation of different variants of the presented method. The three rows of each dataset from top to bottom denote PSNR and SSIM scores, respectively. Bold values show the best performer.

Dataset	Raw	UDCP	ULAP	RGHS	IBLA	CycleGAN	SESR	DAL	Ours
UFO	20.30	14.55	19.07	17.84	17.70	20.01	25.17	19.33	**26.55**
	0.77	0.57	0.73	0.74	0.65	0.82	0.83	0.76	**0.84**
SC	15.54	12.28	17.46	15.82	15.85	18.84	20.52	19.23	**27.85**
	0.73	0.54	0.73	0.72	0.65	0.78	0.79	0.77	**0.87**
IGN	20.91	14.34	19.83	18.30	18.58	19.85	25.67	19.35	**28.31**
	0.77	0.55	0.74	0.75	0.66	0.78	0.86	0.75	**0.87**

4.3Ablation Experiments

We performed ablation experiments on key components of the model in the UIEB underwater image dataset, and the visual comparison results are shown in Figure. 5. As shown in Figure. 5 (b), after removing the adaptive module, the watercolor effect is still present although the model improves the contrast to some extent. Significant edge sharpening and loss of detail can be observed after removing the high-frequency branch, as shown in Figure. 5 (b). As shown in Figure. 5 (c),after removing the low-frequency branch, enhancement result shows blurring and color shift. As shown in Fig. 5 (d), the results of the full model are closest to the ground truth. The average scores of PSNR and SSIM are presented in Table 4. These experiments validate the effectiveness of each component of the model.

5. CONCLUSION

We propose a novel underwater image enhancement network that can adaptively handle the negative effects of different water types on the enhanced images, thus providing a generalized enhancement network. In addition, the proposed dual-layer synchronized enhancement network can learn the feature information of different frequencies underwater,

which leads to a more realistic sensory effect of the enhanced image. Meanwhile, extensive experimental results on real underwater images and synthetic images with different water types show that the method is competitive and generalizable.

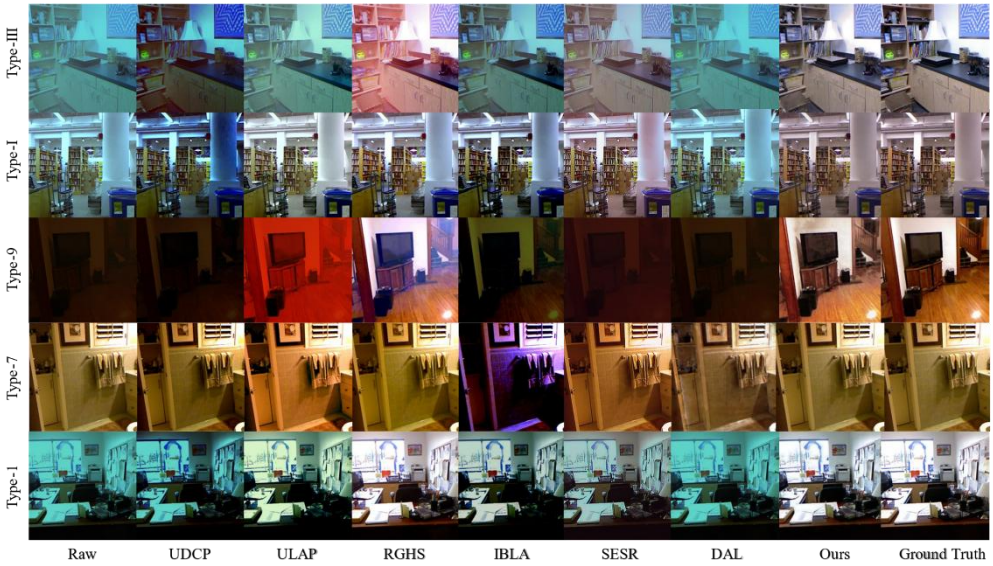

Figure 4. Qualitative comparisons of results on synthetic underwater images.

Table 3: Quantitative comparisons of results on synthetic underwater images. The two lower rows of each type denote PSNR and SSIM scores, respectively. Bold values show the best performer.

Type	Raw	UDCP	ULAP	RGHS	IBLA	CycleGAN	SESR	DAL	Ours
Type-1	13.24	14.50	13.97	13.74	15.02	14.64	15.85	22.98	**26.39**
	0.68	0.70	0.69	0.74	0.68	0.65	0.70	0.82	**0.90**
Type-3	12.86	11.86	12.40	11.30	12.97	14.07	13.95	21.92	**22.59**
	0.62	0.61	0.60	0.66	0.63	0.64	0.60	0.78	**0.85**
Type-5	10.44	9.23	11.02	9.72	10.87	13.07	11.93	21.08	**23.51**
	0.48	0.42	0.53	0.59	0.50	0.63	0.45	0.73	**0.82**
Type-7	8.11	7.74	9.89	8.41	8.82	19.52	9.58	19.73	**18.59**
	0.28	0.22	0.42	0.51	0.30	0.59	0.30	0.66	**0.67**
Type-9	7.59	7.68	8.99	6.86	7.71	10.93	8.57	15.80	**17.49**

	0.19	0.18	0.29	0.44	0.18	0.45	0.22	0.58	**0.59**
Type-I	15.72	17.87	14.61	14.69	9.06	17.10	15.28	24.23	**29.41**
	0.81	0.83	0.76	0.78	0.20	0.74	0.75	0.85	**0.94**
Type-II	15.23	17.10	14.61	14.22	15.00	15.86	16.32	23.59	**27.64**
	0.79	0.81	0.76	0.76	0.65	0.73	0.74	0.84	**0.93**
Type-III	14.06	14.57	13.60	14.74	15.00	15.20	15.92	15.83	**26.80**
	0.72	0.73	0.70	0.75	0.77	0.68	0.71	0.75	**0.91**

Table 4: Ablation experiments for each key component. Bold values show the best performer.

Metric	-AM	-HF branch	-LF branch	Full
PSNR	23.81	22.27	22.06	**25.00**
SSIM	0.90	0.88	0.90	**0.91**

(a) Raw (b) -AM (c) –HF Branch (d) -LF Branch (e) Ours (f) Ground Truth

Figure 5.Ablation experiments for each key component.

REFERENCES

[1]Syed Waqas Zamir, Aditya Arora, Salman Khan, Munawar Hayat, Fahad Shahbaz Khan, and Ming-Hsuan Yang. Restormer: Efficient transformer for high-resolution image restoration. In Proceedings of the IEEE/CVF Conference on Computer Vision and Pattern Recognition, pages 5728–5739, 2022.

[2]AdarshJamadandi and Uma Mudenagudi. Exemplar-based underwater image enhancement augmented by wavelet corrected transforms. In Proceedings of the IEEE/CVF Conference on Computer Vision and Pattern Recognition Workshops, pages 11–17, 2019.

[3]MdJahidul Islam, Peigen Luo, and JunaedSattar. Simultaneous enhancement and super-resolution of underwater imagery for improved visual perception. arXiv preprint arXiv:2002.01155, 2020.

[4]Chongyi Li, ChunleGuo, Wenqi Ren, Runmin Cong, JunhuiHou, Sam Kwong, and Dacheng Tao. An underwater image enhancement benchmark dataset and beyond. IEEE Transactions on Image Processing, 29:4376–4389, 2019.

[5]Pritish M Uplavikar, Zhenyu Wu, and Zhangyang Wang. All-in-one underwater image enhancement using domain-adversarial learning. In CVPR workshops, pages 1–8, 2019.

[6]Lintao Peng, Chunli Zhu, and LihengBian. U-shape transformer for underwater image enhancement. arXiv preprint arXiv:2111.11843, 2021.

[7]Muwei Jian, Xiangyu Liu, Hanjiang Luo, Xiangwei Lu, Hui Yu, and Junyu Dong. Underwater image processing and analysis: A review. Signal Processing: Image Communication, 91:116088, 2021.

[8]Chongyi Li, Saeed Anwar, JunhuiHou, Runmin Cong, ChunleGuo, and Wenqi Ren. Underwater image enhancement via medium transmission-guided multi-color space embedding. IEEE Transactions on Image Processing, 30:4985–5000, 2021.

[9] John Y Chiang and Ying-Ching Chen. Underwater image enhancement by wavelength compensation and dehazing. IEEE transactions on image processing, 21(4):1756– 1769, 2011.
[10] Prasen Kumar Sharma, Ira Bisht, and Arijit Sur. Wavelength-based attributed deep neural network for underwater image restoration. ACM Journal of the ACM (JACM), 2021.
[11] Paul Drews, Erickson Nascimento, Filipe Moraes, Silvia Botelho, and Mario Campos. Transmission estimation in underwater single images. In Proceedings of the IEEE international conference on computer vision workshops, pages 825–830, 2013.
[12] Kaiming He, Jian Sun, and Xiaoou Tang. Single image haze removal using dark channel prior. IEEE transactions on pattern analysis and machine intelligence, 33(12): 2341–2353, 2010.
[13]Saeed Anwar, Chongyi Li, and FatihPorikli. Deep underwater image enhancement. arXiv preprint arXiv:1807.03528, 2018.
[14]Nils Gunnar Jerlov. Marine optics. Elsevier, 1976.
[15]Z. Pan, J. Cai, and B. Zhuang, “Fast vision transformers with hilo attention,” in NeurIPS, 2022.
[16]MdJahidul Islam, SadmanSakibEnan, Peigen Luo, and Junaed Sattar. Underwater image super-resolution using deep residual multipliers. In 2020 IEEE International Conference on Robotics and Automation (ICRA), pages 900–906. IEEE, 2020.
[17]Y. T. Peng and P. C. Cosman. Underwater image restoration based on image blurriness and light absorption. IEEE Trans Image Process, 26(4):1579–1594, 2017.
[18] Paulo LJ Drews, Erickson R Nascimento, Silvia SC Botelho, and Mario Fernando Montenegro Campos. Underwater depth estimation and image restoration based on single images. IEEE computer graphics and applications, 36(2):24–35, 2016.
[19] Wei Song, Yan Wang, Dongmei Huang, and Dian Tjondronegoro. A rapid scene depth estimation model based on underwater light attenuation prior for underwater image restoration. In Pacific Rim Conference on Multimedia, pages 678–688. Springer, 2018.
[20] Dongmei Huang, Yan Wang, Wei Song, Jean Sequeira, and Sébastien Mavromatis. Shallow-water image enhancement using relative global histogram stretching based on adaptive parameter acquisition. In International conference on multimedia modeling, pages 453–465. Springer, 2018.
[21] Jun-Yan Zhu, Taesung Park, Phillip Isola, and Alexei A Efros. Unpaired image-toimage translation using cycle-consistent adversarial networks. In Proceedings of the IEEE international conference on computer vision, pages 2223–2232, 2017.
[22] MdJahidul Islam, Youya Xia, and JunaedSattar. Fast underwater image enhancement for improved visual perception. IEEE Robotics and Automation Letters, 5(2):3227– 3234, 2020.
[23] J. Zhou, L. Pang, D. Zhang and W. Zhang, "Underwater Image Enhancement Method via Multi-Interval Subhistogram Perspective Equalization," in IEEE Journal of Oceanic Engineering, vol. 48, no. 2, pp. 474-488, 2023.
[24] J. Zhou, Y. Wang, C. Li and W. Zhang, "Multicolor Light Attenuation Modeling for Underwater Image Restoration," in IEEE Journal of Oceanic Engineering, vol. 48, no. 4, pp. 1322-1337, Oct. 2023.
[25] G. Hou, N. Li, P. Zhuang, K. Li, H. Sun and C. Li, "Non-Uniform Illumination Underwater Image Restoration via Illumination Channel Sparsity Prior," in IEEE Transactions on Circuits and Systems for Video Technology, vol. 34, no. 2, pp. 799-814, Feb. 2024
[26] Wang, Zhou, et al. “Image quality assessment: from error visibility to structural similarity,” IEEE transactions on image processing, vol. 13, no. 4 pp. 600 – 612, 2004.
[27] Korhonen, Jari, and Junyong You. “Peak signal-to-noise ratio revisited: Is simple beautiful?, ” Proceedings of the 2012 Fourth International Workshop on Quality of Multimedia Experience. pp.38 – 38, 2012.